1995108046

N95-14460

S07-39

23101

P- 14

David Broek
FractuREsearch, Inc.
Galena, OH 43021 USA

David Y. Jeong
U.S. Department of Transportation
Research and Special Programs Administration
Volpe National Transportation Systems Center
Cambridge, MA 02142 USA

Douglas Thomson
Foster-Miller, Inc.
Waltham, MA 02154 USA

SUMMARY

An experimental and analytical investigation of multiple cracking in various types of test specimens is described in this paper. The testing phase is comprised of a flat unstiffened panel series and curved stiffened and unstiffened panel series. The test specimens contained various configurations for initial damage. Static loading was applied to these specimens until ultimate failure, while loads and crack propagation were recorded. This data provides the basis for developing and validating methodologies for predicting linkup of multiple cracks, progression to failure, and overall residual strength.

The results from twelve flat coupon and ten full scale curved panel tests are presented. In addition, an engineering analysis procedure was developed to predict multiple crack linkup. Reasonable agreement was found between predictions and actual test results for linkup and residual strength for both flat and curved panels. The results indicate that an engineering analysis approach has the potential to quantitatively assess the effect of multiple cracks on the arrest capability of an aircraft fuselage structure.

INTRODUCTION

Multiple cracking has been observed in several airplanes that have been in service for sometime. The term "Widespread Fatigue Damage" (WFD) is commonly used to refer to a type of multiple cracking that degrades the damage tolerance capability of an aircraft structure. Laboratory testing of flat [1] and curved panels [2] has demonstrated that residual strength is reduced when a lead crack is accompanied by several smaller collinear cracks, compared to the case of a single lead crack only. Moreover, the in-flight failure of the fuselage of Aloha Airlines Flight 243 in 1988 is believed to have been caused by the linking of multiple cracks [3] and the associated degradation of the structure's crack arrest capability.

The Federal Aviation Administration Technical Center (FAATC) has initiated several research programs to investigate the effect of multiple cracking on the structural integrity of the aging fleet. One area of research is to quantify the reduction of residual strength due to multiple cracking in various aircraft components. Analytical predictions of residual strength, however, require the application of appropriate criteria to determine coalescence or linkup of multiple cracks. Swift [4] has hypothesized that a lead crack will linkup with smaller, collinearly aligned cracks when the plastic zones from adjacent crack tips join together. Other linkup criteria, such as the crack tip opening angle [5], have also been proposed, but a generally accepted criterion for multiple crack linkup has not been established.

A test program was designed by FractuREsearch, Inc. [6], and implemented by Foster-Miller, Inc., under contract with the John A. Volpe National Transportation Systems Center, to generate data which could be used to validate results from analytical models. These data are especially appropriate for verification of proposed multiple crack linkup criteria. This paper summarizes the test program and some of the analyses that were performed to correlate the experimental data with linkup predictions. Additional details of the experimental and the analytical phases of this work can be found in References [6], [7] and [8].

EXPERIMENTAL PROGRAM

The Foster-Miller test program may be divided into 3 separate series: (1) basic coupon testing, (2) flat panel testing, and (3) curved panel testing. Thus, the test specimen in each test series had an increased level in complexity as testing progressed. The material of the panels in each test series was 2024-T3 alclad aluminum.

Basic Coupon Tests

The first series of tests was conducted on 1-inch wide coupons to determine basic material properties of 2024-T3 alclad aluminum. Nine (9) coupons were used with varying skin thickness and grain orientation. Average values of yield strength, ultimate strength, and percent elongation for each coupon combination are listed in Table 1.

Table 1. Mechanical Properties of 2024-T3 Aluminum.

Direction/ Thickness (inch)	Yield Strength (ksi)	Ultimate Strength (ksi)	Percent Elongation
Longitudinal/0.040	51.9	64.4	13.9
Transverse/0.040	43.7	63.8	13.7
Transverse/0.080	44.1	66.6	13.8

Flat Panel Tests

The flat panel series was comprised of 12 panels with various multiple crack configurations, shown schematically in Figure 1. These flat panels were unstiffened, with a width of 20 inches and thickness of 0.040 inch. The first three panels contain single cracks only, while the other nine contain a lead crack with one, two or three smaller collinear cracks ahead of each crack tip. Figure 1 also lists the stresses at linkup and at failure for each panel. In some cases, panel failure and linkup occurred simultaneously. For example, the stress at failure in Panel 7 coincides with the stress at linkup for all three ligaments.

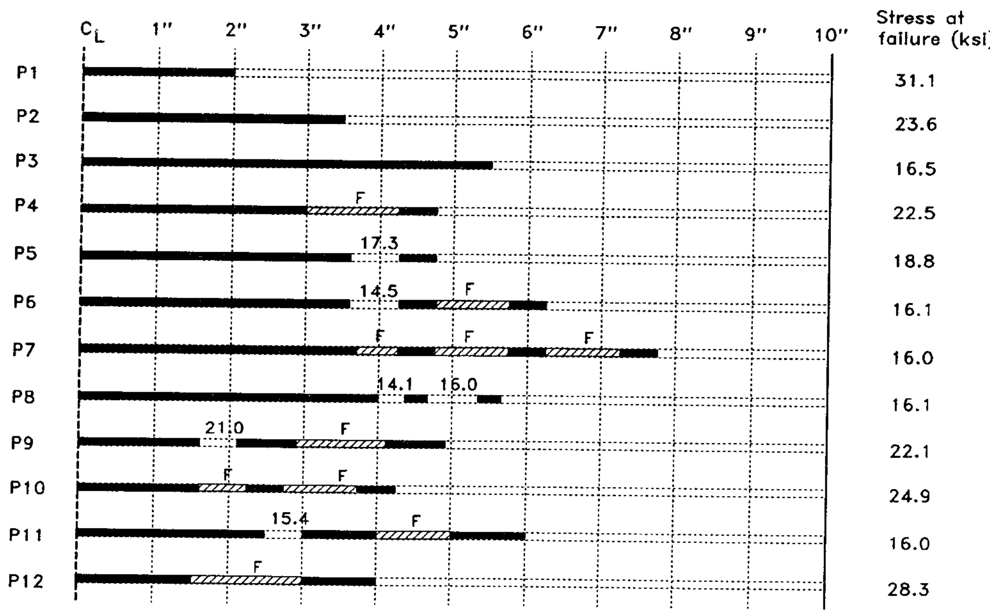

Figure 1. Summary of flat panel tests.

Curved Panel Tests

The full-scale test facility designed and built by Foster-Miller, Inc. was utilized in the curved panel test series. A description of this unique facility can be found in References [2] and [9].

Both unstiffened and stiffened panels were used in this series. The panels have a radius of curvature of 75 inches. The dimensions of the panel test section are 68 inches along the circumference by 120 inches along the width. The curved panels were made from the same batch of 0.040-inch thick 2024-T3 alclad aluminum as the flat panels. Three unstiffened curved panels were tested. The crack configurations for these panels are shown schematically in Figure 2. Six (6) stiffened curved panels were tested. Crack arresters in the form of tear straps were attached to the skin by two columns of rivets as well as an adhesive bond. Two different tear strap designs, referred to as "light" and "heavy" were used - 4 panels had "light" tear straps and 2 with "heavy" tear straps (see Figure 3). Table 2 lists the relevant dimensions of these two tear strap designs.

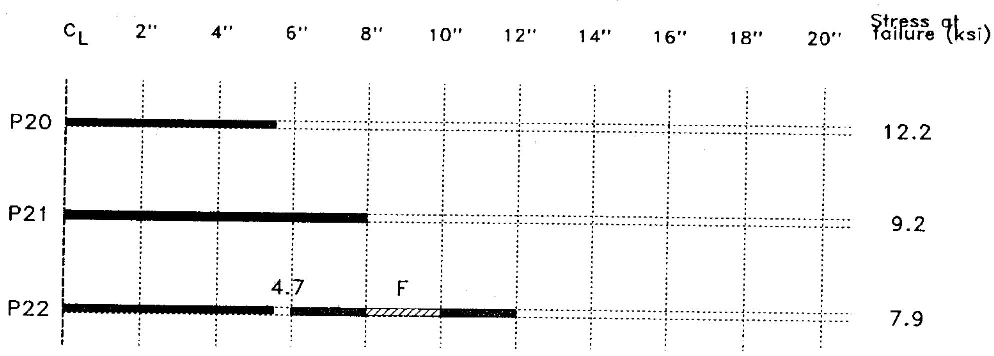

Figure 2. Summary of unstiffened curved panel tests.

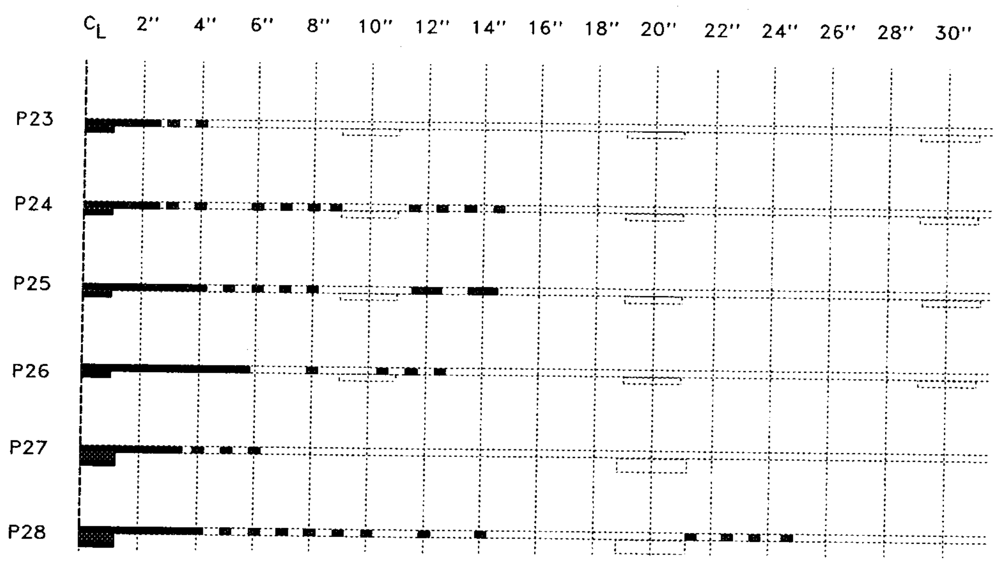

Figure 3. Summary of stiffened curved panel tests.

Table 2. Dimensions of Tear Strap Designs

	Light	Heavy
Thickness (inch)	0.04	0.08
Width (inches)	2.00	2.50
Cross sectional area (inch^2)	0.08	0.20
Longitudinal spacing (inches)	10.0	20.0

CORRELATION OF TEST DATA WITH ANALYSIS

Swift's criterion [4] for linkup of multiple cracks can be expressed mathematically as

$$r_p(a) + r_p(b) = L \tag{1}$$

where $r_p(a)$ and $r_p(b)$ refer to the extent of the plastic zones ahead of the two adjacent cracks and L is the distance between crack tips or the ligament length (Figure 4). Note that in Figure 4, the lead or main crack has a total length of $2a$, while the length of the smaller crack is $2b$. One approach[1] to determine the extent of crack tip plasticity is to use the Dugdale equation [10]:

$$r_p = \frac{\pi}{8}\left(\frac{K_I}{\sigma_p}\right)^2 \tag{2}$$

where σ_p is the yield strength of the material. Also, K_I is the stress intensity factor which can be written as

$$K_I = \sigma_o \beta \sqrt{\pi a} \tag{3}$$

where σ_o is the far field stress and β is a geometric correction factor that accounts for effects such as crack interaction, finite width, and crack face bulging.

---

1 References [6] and [8] describe other models that can be used to determine the size of the plastic zone ahead of the crack tip.

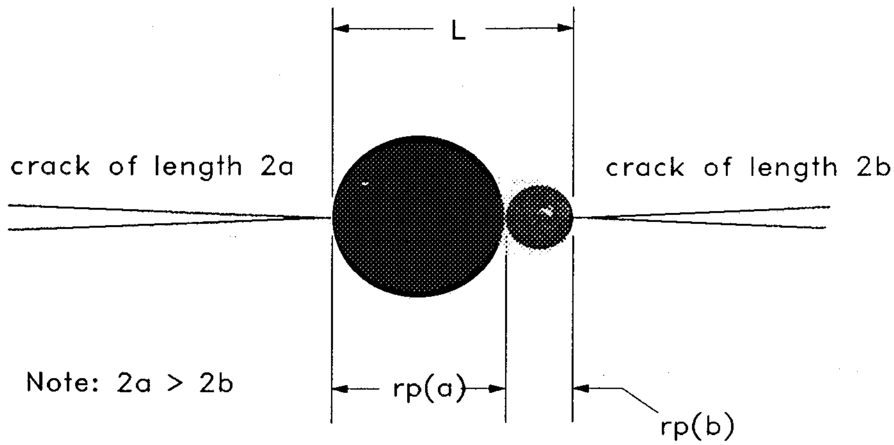

Figure 4. Schematic of linkup criterion based on plastic zone size.

The far field stress at linkup can be determined by combining equations (1), (2), and (3):

$$\sigma_o = \sigma_p \sqrt{\frac{8L}{\pi^2[\beta(a)^2 a + \beta(b)^2 b]}} \quad . \tag{4}$$

The correction factors for crack interaction, $\beta(a)$ and $\beta(b)$, can be found in handbooks such as Reference [11]. Predictions for multiple crack linkup have been made using equation (4) assuming the yield strength of 2024-T3 aluminum to be 50 ksi. Table 3 compares linkup predictions with the experimental results for the various flat panels. On average, the predictions overestimate the actual linkup stresses by 4.7%. The accuracy of the linkup predictions appears to be affected by the ligament length; the percent difference between predicted stresses and test data increases with ligament length.

Predictions for multiple crack linkup can be modified to include the effect of stable tearing [12]. Stable tearing affects the linkup analysis by reducing the distance between cracks which also increases the stress intensity factors due to interaction. The amount of stable tearing can be calculated using the following two-parameter R-curve equation that was derived from a regression analysis of the flat panel test data:

$$K_R = 106.1 \Delta a^{0.212} \tag{5}$$

When the effect of stable tearing is included in the analysis, an iterative procedure must be used to solve equation (4) because the distance between crack tips, L, depends on the amount of stable tearing, Δa, which is a function of the far field stress, σ_o. Table 3 also lists the linkup predictions when stable tearing is included in the analysis. Predictions with stable tearing included are within 2% of the experimental data, on average.

Table 3. Correlations Between Flat Panel Test Data and Analysis

(a) First Linkup

Specimen	Crack Dimensions (inches)			Prediction σ_o (ksi) and Percent Difference from Test Result				Test Result
	a	b	L	*NO Stable Tearing*		*With Stable Tearing*		σ_{EXP} (ksi)
P4	3.00	0.25	1.25	26.8	+18.9%	23.8	+5.9%	**22.5**
P5	3.60	0.25	0.65	17.0	-2.0%	16.1	-6.8%	**17.3**
P6	3.80	0.25	0.45	13.3	-8.6%	12.9	-11.3%	**14.5**
P7	3.70	0.25	0.55	15.2	-5.2%	14.6	-9.0%	**16.0**
P8	4.00	0.15	0.35	11.8	-16.1%	11.6	-18.0%	**14.1**
P9	1.60	0.40	0.50	19.3	-8.1%	18.8	-10.7%	**21.0**
P10	1.60	0.25	0.65	24.7	+1.0%	23.4	-5.9%	**24.9**
P11	2.50	0.50	0.50	15.2	-1.5%	14.8	-4.2%	**15.4**
P12	1.50	0.50	1.50	36.8	+30.1%	32.8	+15.8%	**28.3**

(b) Second Linkup

Specimen	Crack Dimensions (inches)			Prediction σ_o (ksi) and Percent Difference from Test Result				Test Result
	a	b	L	*NO Stable Tearing*		*With Stable Tearing*		σ_{EXP} (ksi)
P6	4.75	0.25	1.00	19.0	+18.1%	17.4	+8.3%	**16.1**
P8	4.65	0.15	0.70	16.3	+2.2%	15.4	-3.8%	**16.0**
P9	2.90	0.40	1.20	25.3	+14.6%	22.9	+3.8%	**22.1**
P11	4.00	0.50	1.00	19.1	+19.2%	17.7	+10.5%	**16.0**

Pressurization of a curved panel containing a longitudinal crack creates in-plane and out-of-plane deformations of the crack faces which is generally referred to as bulging. Physically, crack face bulging causes local bending at the crack tips which increases the effective stress intensity factor. In an engineering analysis, the stress intensity factor for a curved panel can be calculated by multiplying the stress intensity factor for a flat panel by an appropriate bulging factor. Thus, the same approach used to predict multiple crack linkup in flat panels can be applied to curved panels if the bulging factor is known. The following bulging factor was used in the subsequent analyses of curved panels [13]:

$$\beta_B = \sqrt{1 + \alpha\left[\left(\frac{E}{\sigma_o}\right)\left(\frac{a}{R}\right)^2\right]^{\frac{2}{3}}} \tag{6}$$

where E is the modulus of elasticity of the panel material (10 msi), σ_o is the far field stress, a is the half-crack length, R is the radius of curvature (75 inches), and α is an empirical constant (0.671)[2]. This bulging factor was derived by assuming that the R-curve data for unstiffened flat and curved panels is the same [13]. The applicability of other bulging factors is also discussed in Reference [13].

Table 4 lists the linkup predictions for curved unstiffened panels based on using Swift's criterion [4] with the Dugdale plastic zone model and equation (6) for the bulging factor. The yield strength of 2024-T3 alclad aluminum was assumed to be 50 ksi. The agreement between test data and analysis is reasonable, and improves when the effect of stable tearing is included.

Table 4. Correlations Between Unstiffened Curved Panel Test Data and Analysis

	Crack Dimensions (inches)			Prediction σ_o (ksi) and Percent Difference from Test Result				Test Result
	a	b	L	*NO Stable Tearing*		*With Stable Tearing*		σ_{EXP} (ksi)
1st Linkup	5.50	1.00	0.50	5.0	+6.4%	4.8	+2.1%	**4.7**
2nd Linkup	8.00	1.00	2.00	9.9	+25.3%	7.3	-7.6%	**7.9**

2 The numbers in parentheses refer to the values assumed in the analysis.

Analyses were also performed to account for the effect of stiffening in curved panels due to tear straps. Stiffening affects the calculation of the stress intensity factor and the bulging factor. A displacement compatibility approach [14] was employed to calculate stress intensity factors in cracked stiffened panels. This approach can be used to account for such effects as rivet flexibility, biaxial stress, and broken or intact center stiffeners. Rivets are modelled as springs with linear flexibility in the circumferential direction[3]. Swift [15] has derived an empirical formula to calculate the linear flexibility $(1/k)$ of aluminum rivets:

$$\frac{1}{k} = \frac{1}{Ed}\left[5.0 + 0.8d\left(\frac{1}{t_1} + \frac{1}{t_2}\right)\right] \tag{7}$$

where E is the modulus of elasticity of the sheet material, t_1 and t_2 are the thicknesses of the joined sheets, and d is the rivet hole diameter.

Since the displacement compatibility method calculates stress intensity factors for a flat, cracked, stiffened panel, an appropriate bulging factor must be assumed. In the present analysis, equation (6) was modified by using a damping factor that was proposed by Swift [16]. This damping factor assumes that bulging is greatest at midbay, and is minimized at the stiffener locations. Thus, the following bulging factor was used to account for stiffening:

$$\beta_B = \sqrt{1 + \alpha\left[\left(\frac{E}{\sigma_o}\right)\left(\frac{a}{R}\right)^2\right]^{\frac{2}{3}}\left[1 - \cos\left(\frac{2\pi a}{L}\right)\right]} \tag{8}$$

where L is the tear strap spacing (from Table 2, this spacing is 10 inches for light tear straps and 20 inches for heavy tear straps).

Table 5 lists the results from the correlations between analytical predictions and test data for curved panels. While most of these panels contained more than two cracks (recall Figure 3), only the first two linkup stresses are included in Table 5 for brevity. The effect

3 Nonlinear rivet flexibility can also be modelled in the displacement compatibility approach by implementing an iterative solution procedure and a piecewise linear flexibility curve.

of stable tearing has been included in the analytical predictions listed in Table 5. In general, the agreement between analysis and experiment for linkup stress is good. The engineering analysis predicts linkup stresses with 10% of the test results in the cases where the ligament length is less than 0.5 inch. When the distance between cracks is 0.5 inches or greater, the linkup predictions differ from the test result by more than 20%. These differences are comparable to those observed in the flat correlations. In terms of overall panel failure, predictions for panels with light tear straps are within 25% of the experimental results. Predictions for panels with heavy straps overestimate the observed values by as much as 77%. Considering the uncertainty associated with the bulging factor, the general trend of the results produced by the engineering approach described in this paper appears encouraging.

Table 5. Correlations Between Curved Panel Test Data and Analysis (Far field stress, in ksi)

Panel	First Linkup			Second Linkup			Panel Failure		Comments
	Predict	*Test*	L(a)	*Predict*	*Test*	L(a)	*Predict*	*Test*	
22	4.8	**4.7**	0.5	7.3	**7.9**	2.0	7.3	**7.9**	Unstiffened
23	10.6	**11.3**	0.2	11.9	**15.2**	0.6	23.1	**22.1**	Light tear straps
24	10.6	**11.3**	0.2	11.9	**15.2**	0.6	20.9	**18.0**	Light tear straps
25	11.4	**11.1**	0.	11.4	**11.1**(b)	0.6	21.1	**16.9**	Light tear straps
26	-	N/A	-	-	N/A	-	15.9	**16.9**(b)	Light tear straps
27	10.9	**10.9**	0.3	12.4	**11.8**	0.6	20.0	**13.3**(d)	Heavy tear straps
28	11.9	**9.9**	0.5	11.9	**9.9**	0.6	17.5	**9.9**	Heavy tear straps

NOTES:

(a) L = Ligament length or distance between cracks (in inches).

(b) Stress at linkup for first 4 ligaments.

(c) Initially, test was conducted with INTACT center stiffener. The test was restarted after the center stiffener was intentionally cut.

(d) Test fixture ran out of stroke before panel failure. Therefore, the recorded failure pressure is probably too low.

CONCLUSIONS

(1) Tests on 20-inch wide, flat, unstiffened panels demonstrated that residual strength is reduced when a lead crack is accompanied by several smaller, collinear cracks.

(2) Using Swift's proposed criterion for multiple crack linkup [4] and Dugdale's plastic zone model, predictions can be obtained to give reasonable agreement with experimental data. Predictions of multiple crack linkup for flat panels averaged within 5% of the experimental data.

(3) The effect of stable tearing can be included in predictions of multiple crack linkup by using an iterative solution procedure. Using the Dugdale plastic zone model, predictions of linkup in flat panels averaged within 2% of the experimental data when stable tearing was included.

(4) Ligament length or distance between crack tips appears to affect the accuracy of predictions for multiple crack linkup. Predictions are more accurate when the ligament length is less than 0.5 inches.

Acknowledgement - The research described in this paper was performed in support of the Federal Aviation Administration Technical Center's Aging Aircraft Research Program. The support and interest from Dr. Michael L. Basehore at FAATC is gratefully appreciated by the authors.

REFERENCES

[1] Maclin, J.R.: Performance of Fuselage Pressure Structure, *1991 International Conference on Aging Aircraft and Structural Airworthiness,* NASA CP-3160, Washington, D.C., 1992, pp. 67-75.

[2] Samavedam, G.; Hoadley, D.; and Thomson, D.: Full-Scale Testing and Analysis of Curved Aircraft Fuselage Panels, Final Report, DOT/FAA/CT-93/78, DOT-VNTSC-FAA-93-10, December 1993.

[3] National Transportation Safety Board: Aircraft Accident Report - Aloha Airlines, Flight 243, Boeing 737-200, N737-200, N73711, near Maui, Hawaii, April 28, 1988, NTSB/AAR-89/03, PB89-910404, June 1989.

[4] Swift, T.: Damage Tolerance Capability, *Specialists Conference on Fatigue of Aircraft Materials,* Delft University of Technology, October 1992.

[5] Newman, J.C.; Dawicke, D.S.; Sutton, M.A.; and Bigelow, C.A.: A Fracture Criterion for Widespread Cracking in Thin-Sheet Aluminum Alloys, *17th ICAF Symposium on Durability and Structural Integrity of Airframes,* Stockholm, Sweden, June 1993.

[6] Broek, D.: The Effects of Multi-Site Damage on the Arrest Capability of Aircraft Fuselage Structures, FractuREsearch Report No. TR 9302, June 1993.

[7] Thomson, D.; Hoadley, D.; and McHatton, J.: Load Tests of Flat and Curved Panels with Multiple Cracks, Foster-Miller Draft Final Report to Volpe Center, September 1993.

[8] Jeong, D.Y.: Analysis of Residual Strength Tests on Flat and Curved Panels with Multiple Cracks, Volpe Center Draft Final Report, October 1993.

[9] Samavedam, G.; and Hoadley, D.: Fracture and Fatigue Strength Evaluation of Multiple Site Damaged Aircraft Fuselages - Curved Panel Testing and Analysis, Final Report, DOT/FAA/CT-94/10, DOT-VNTSC-FAA-93-8, January 1994.

[10] Dugdale, D.S.: Yielding of Steel Plates Containing Slits, *Journal of the Mechanics and Physics of Solids 8,* 1960, pp. 100-108.

[11] Tada, H.; Paris, P.; and Irwin, G.: *The Stress Analysis of Cracks Handbook,* Second Edition, Paris Productions, Inc., 1985.

[12] Tong, P.; Greif, R.; Chen, L.; and Jeong, D.Y.: Damage Tolerance of Fuselage Panels with Widespread Fatigue Damage, *17th ICAF Symposium on Durability and Structural Integrity of Airframes,* Stockholm, Sweden, June 1993.

[13] Jeong, D.Y.; and Tong, P.: Nonlinear Bulging Factor Based on R-Curve Data, *FAA/NASA International Symposium on Advanced Structural Integrity Methods for Airframe Durability and Damage Tolerance*, NASA CP-3274, 1994.

[14] Swift, T.: The Effects of Fastener Flexibility and Stiffener Geometry on the Stress Intensity Factor in Stiffened Cracked Sheet, *Prospects of Fracture,* Noordhoff International, Leyden, The Netherlands, 1974, pp. 419-536.

[15] Swift, T.: Development of the Fail-Safe Design Features of the DC-10, *Damage Tolerance in Aircraft Structures, ASTM STP 486,* American Society for Testing and Materials, Philadelphia, PA, 1971, pp. 164-214.

[16] Swift, T.: Design of Redundant Structures, *Fracture Mechanics Design Methodology,* AGARD-LS-97, North Atlantic Treaty Organization, London, England, 1979.